

NEW ANALYTICAL SOLUTION OF THE NONLINEAR DYNAMIC FLOOD WAVE EQUATION IN RIVERS

Ela Doganay¹ and Sergio E. Serrano²

ABSTRACT

The authors present additional independent verification and a validation of the new approximate analytical solution to the nonlinear kinematic wave equation (Serrano, 2006), and the new analytical solution to the nonlinear dynamic wave equation in rivers (Serrano, 2016). Specifically, the new solutions are compared with independent simulations using the modified finite-element method and with field data at the Schuylkill River near Philadelphia for the hydrologic year of 2004. The new solutions are further validated in the same watershed, without changing the parameters, for the hydrologic years of 2011 and 2012, when Hurricane Irene and Hurricane Sandy, respectively, touched down in the region. The new solutions compared favorably. The solutions have been derived by combining Adomian's Decomposition Method (ADM), the method of characteristics, the concept of double decomposition, and successive approximation. The new analytical solutions are easy to apply, permit an efficient preliminary forecast under scarce data, and an analytic description of flow rates continuously over the spatial and temporal domains. They may also serve as a potential source of reference data for testing new numerical methods and algorithms proposed for the open channel flow equations. The ADM nonlinear kinematic and nonlinear dynamic wave solutions exhibit the usual features of nonlinear hydrographs, namely their asymmetry with respect to the center of mass, with sharp rising limbs and flatter recession limbs. Linear methods usually miss these characteristics. The greatest portion of the magnitude of discharge is given by the initial nonlinear kinematic wave component, which implies that in the lower Schuylkill river the translational components dominate the propagation of flood waves, in agreement with previous research. The nonlinear dynamic wave better predicts the flow rate, during peak times and especially during recession and low-flow periods. Thus, while the new approximate analytical solutions to the nonlinear kinematic and the nonlinear dynamic wave models are easier to implement than numerical solutions, the nonlinear kinematic wave equation model requires less data and less computational effort. This article presents, to our knowledge, the first analytical solution to this complex problem. It overcomes most restrictions of existing numerical models (e.g., no need for a grid, specialized software, complex discretization, special smoothing of the front wave end, small perturbation, numerical instability, linearization, replacement of momentum equation by empirical relationships, etc.). It represents a physically-based solution of the true nonlinear combined mass and momentum equations. The flood wave is continuous in space and time. Its implementation is extremely simple with any standard mathematics program (e.g., Matlab).

Keywords: Nonlinear kinematic and dynamic flood waves, analytical solutions, mathematical models, Adomian's Decomposition Method.

INTRODUCTION

The propagation of flood waves in rivers is governed by the nonlinear Saint Venant equations. Under certain simplified assumptions, many models have been developed over the last several decades (e.g., de Almeida, and Bates, 2013; de Almeida et al., 2012; Philipp et al., 2012; Bates et al., 2010; Moramarco et al., 2008; Tsai and Yen, 2004; Tsai, 2003; Aronica et al., 1998; Cappelaere, 1997; Lamberti and Pilati, 1996; Singh and Aravamathan, 1996; Xia, 1995; Dooge and Napiorkowski, 1987; Hromadka and Yen, 1986; Ponce, 1986; Ferrick, 1985; Ferrick et al., 1984; Vieira, 1983; Morris and Woolhiser, 1980; Ponce et al., 1978; Ponce and Simons, 1977; Di Silvio, 1969; Woolhiser and Liggett, 1967; Lighthill and Whitham, 1955). Most approaches to solve the resulting nonlinear equations use numerical methods or analytical solutions of the linearized equations (e.g., Kazezyilmaz-Alhan and Medina, 2007; Jin and Fread, 1997). Recent refinements in the linear

¹ Graduate Student, Dept. of Civil Engineering, Temple University, Philadelphia, PA 19122

² Professor Emeritus, Temple University, Philadelphia, PA 19122, sserrano@temple.edu

approximations of the flood routing equations successfully simulate the nonlinear features of flood waves. Examples of these approaches include the variable parameter Muskingum-Cunge method (Ponce and Chaganti, 1994), the variable parameter Muskingum-Cunge-Todini method (Todini, 2007) and the variable parameter Muskingum-Price method (Price, 2009). In addition, these methods also implement various approaches to overcome the loss of mass conservation inherent in nonlinear versions of the Saint Venant equations (Reggiani et al., 2014). The variable parameter Muskingum methods satisfy mass conservation only, since the momentum conservation equation is replaced by empirical equations. The resulting equations are solved via complex numerical procedures that require finite difference schemes, small perturbation assumptions, optimization, and stability control of spatial and temporal intervals (e.g., Reggiani et al., 2014; Price 2009).

There is a cogent need for analytical solutions of the nonlinear kinematic wave and the nonlinear dynamic wave equations in rivers for preliminary analyses under scarce data, and for verification of numerical models. Most approaches reported in the literature use numerical solutions of the relevant equations. Compared to analytical solutions, numerical solutions yield the state variables at discrete nodes only (i.e., they require a grid), are computationally intensive, are difficult to program (i.e., they require specialized computer software), and often have difficulties with numerical instabilities and roundoff errors. There exists a tacit belief that the only possible way to solve a nonlinear equation is to linearize it, to solve it numerically (i.e., numerical linearization), or both. Until recently, linearization of most problems was adopted in order to make the equations tractable with the existing linear methods of solution. Recent advances in applied mathematics have produced new systematic analytic methods of solution to nonlinear equations. They have opened the way to revisit the true nonlinear behavior of many physical systems. One of the few analytical solutions of the nonlinear kinematic wave was proposed by Serrano (2006). This work was discussed by Litrico and Guinot (2007), who presented an alternative solution that required linearization, the introduction of new arbitrary parameters, small perturbation assumptions, and numerical optimization. Litrico and Guinot (2007) is a good linear model. However, an analytical solution to the true nonlinear equation, if available, is easier to implement in many practical scenarios. This discussion was limited to the kinematic wave equation, which is only one aspect of the dynamic wave presented in this paper. Without repeating the details here, this discussion and its subsequent closure (Serrano, 2007) exemplifies the point view of numerical modeling: An objection to physically-based nonlinear models and analytical solutions, in favor of linearized models, empirical equations, small perturbation, and complex numerical solutions. There is no resolution to this philosophical debate. In our view, an analytical solution to an equation, if available, is easier than a numerical solution to the same equation. Indeed, many complex problems with large sets of data available only admit a numerical solution. Also, until now linearization and numerical discretization were justified in the absence of appropriate analytical methods to solve nonlinear equations. In the absence of data in many practical scenarios, and with the advent of new analytical solutions to physically-based nonlinear equations, the need for linearization and complex numerical methods is unjustified. In the spirit of science, we should endeavor to develop mathematical methods that consider the true nonlinear behavior of nature, rather than force nature to conform to the limitations of a favorite method.

In the present work, we use Adomian's Decomposition Method (ADM) (Adomian, 1994, 1991, 1986, 1983), which offers the simplicity, stability, and spatial and temporal continuity of analytical solutions, in addition to the ability to handle system nonlinearities of numerical solutions. For a detailed introduction of the ADM, practical examples in hydrology, and computer programs, see Serrano (2011, 2010). Many studies have reported new solutions to a wide class of equations (ordinary, partial, differential, integral, integro-differential, linear, nonlinear, deterministic or stochastic) in a variety of fields of mathematical physics, science, and engineering (see, for example, Rach, Wazwaz, and Duan, 2013; Duan and Rach, 2011; Rach, 2012, 2008; Wazwaz, 2000; Adomian, 1994, 1991). For nonlinear equations in particular, decomposition is one of the few systematic solution procedures available (Adomian, 1994).

The present work presents a verification of a new set of approximate solutions to the nonlinear kinematic wave (Serrano, 2006) and the nonlinear dynamic wave equations (Serrano, 2016). As such, it attempts to motivate hydrologists to study this problem under the light of new advances in nonlinear science. It does not pretend to solve all the problems inherent

to the Saint Venant equations. For example, it has been known for a long time that the nonlinear kinematic wave equation and the nonlinear dynamic wave equation do not always satisfy either mass conservation or momentum conservation. It is a common problem of most nonlinear transport equations in general. This is because the integration of the local nonlinear equations over spatial and temporal domains yields missing boundary fluxes. This is part of a larger problem in scientific hydrology. The search for appropriate closure relations of hydrologic fluxes has been declared a major challenge of hydrology of the 21st century (Beven, 2006, 2001).

In the following sections, we extend the work of Serrano (2006), who used a one-term ADM expansion to derive an approximate analytical solution to the nonlinear kinematic wave equation, after both acceleration and pressure terms in momentum equation were neglected and the frictional slope was equated to the channel slope. We introduce several mathematical modifications to derive a new approximate analytical solution to the nonlinear kinematic wave equation. Instead of a one-term decomposition, we used the method of double decomposition, and several terms, not just one. In addition, the new solution to the nonlinear kinematic wave equation is used as a first term in the solution to the nonlinear dynamic wave decomposition expansion (Serrano, 2016). The dynamic wave equation includes the acceleration and pressure terms in the momentum equation. The new solutions are compared with independent simulations (Szymkiewicz, 2010) using the modified finite-element method, and with field data at the Schuylkill River near Philadelphia for the hydrologic year of 2004. The new solutions are further validated in the same watershed, without changing the parameters, for the hydrologic years of 2011 and 2012, when Hurricane Irene and Hurricane Sandy, respectively, touched down in the region.

ANALYTICAL SOLUTION OF THE NONLINEAR KINEMATIC AND THE NONLINEAR DYNAMIC WAVE EQUATIONS

Under certain simplifying assumptions of the flow process in rivers, the Saint Venant equations have been solved via traditional numerical methods. The most important assumptions are the following: The flow is one dimensional. Water depth and velocity vary only in the longitudinal direction. This implies that the velocity is constant and the water surface is horizontal across any section perpendicular to the longitudinal axis. Flow is assumed to vary gradually along the river channel. Vertical momentum and vertical accelerations are neglected so that hydrostatic pressure prevails. The longitudinal axis of the river channel is approximated as a straight line. The bottom slope of the channel is small and the channel bed is fixed; the effects of scour and deposition are negligible. Resistance coefficients for steady uniform turbulent flow are applicable. The fluid is incompressible and of constant density throughout the flow. Under these assumptions, detailed derivations of the conservation and non-conservation form of the Saint Venant equations may be consulted in standard treatises. See, for example, Szymkiewicz (2010), Martin and McCutcheon (1999); Chow et al. (1988), and Singh (1996) for excellent descriptions and bibliographic summaries of solution approaches. The conservation form of the continuity equation is given by

$$\frac{\partial Q}{\partial x} + \frac{\partial A}{\partial t} = Q_L \quad (1)$$

where $Q(x,t)$ is the flow rate (L^3/T); Q_L is the lateral flow into the channel per unit length (L^2/L); x is the distance from a streamflow station with a known hydrograph (L); t is time (T); and A is the flow cross-sectional area (L^2). Neglecting the wind shear, eddy losses, and the momentum of lateral flow, the conservation form of the momentum equation is given by (Chow et al, 1988)

$$\frac{1}{A} \frac{\partial Q}{\partial t} + \frac{1}{A} \frac{\partial}{\partial x} \left(\frac{Q^2}{A} \right) + g \frac{\partial y}{\partial x} - g(S_0 - S_f) = 0 \quad (2)$$

where y is the water depth (L); g is the gravitational acceleration (L/T^2); S_0 is the channel bottom slope; and S_f is the slope of the energy line. We initially consider a rectangular channel. Assuming Manning's formula is valid, the following expressions are useful (Chow, 1959):

$$y = \frac{A}{B}, \quad S_f = \frac{n^2 Q^2}{R^{4/3} A^2} = \frac{n^2 (B + 2A/B)^{4/3} Q^2}{A^{10/3}} \quad (3)$$

where B is the channel width at the water surface (L); n is Manning's roughness coefficient; and R is the hydraulic radius (L). Neglecting hysteresis, the channel cross-sectional area is often expressed as

$$A = \alpha Q^\beta \quad (4)$$

where α is a constant with dimensions ($L^{2-3\beta} L^\beta$); and β is a dimensionless constant. Combining (1) and (2), and substituting (3) and (4) into the resulting equation yields a dynamic wave equation given by

$$L_x Q = Q_L - \alpha \beta Q^{\beta-1} L_t Q + S_0 - \frac{n^2}{\alpha^{10/3}} (B + 2\alpha Q^\beta/B)^{4/3} Q^{2-10\beta/3} - \frac{\alpha}{B} L_x Q^\beta - \frac{(2-\beta)}{2g\alpha^2(1-\beta)} L_x Q^{2-2\beta} - \frac{1}{g\alpha Q^\beta} L_t Q, \quad (5)$$

$$Q(0,t) = Q_I(t), \quad Q(x,0) = Q_I(0)$$

where the operators $L_x = \partial/\partial x$, $L_t = \partial/\partial t$; and $Q_I(t)$ is the inflow hydrograph at $x=0$. An x -partial decomposition expansion may be obtained by operating with $L_x^{-1} = \int(\)dx$ on both sides of (5):

$$Q = Q_L x - L_x^{-1} F(Q) L_t Q + L_x^{-1} G(Q) + H(Q) + K(Q) + L_x^{-1} J(Q) L_t Q \quad (6)$$

where the nonlinear functions

$$\begin{aligned} F(Q) &= \alpha \beta Q^{\beta-1} \\ G(Q) &= S_0 - \frac{n^2}{\alpha^{10/3}} (B + 2\alpha Q^\beta/B)^{4/3} Q^{2-10\beta/3} \\ H(Q) &= -\frac{\alpha}{B} Q^\beta \\ K(Q) &= -\frac{(2-\beta)}{2g\alpha^2(1-\beta)} Q^{2-2\beta} \\ J(Q) &= -\frac{1}{g\alpha Q^\beta} \end{aligned} \quad (7)$$

We now define the decomposition series $Q = \sum_{i=0}^{\infty} Q_i$ and the Adomian polynomials for the nonlinear functions in (7) as $F(Q) = \sum_{j=0}^{\infty} F_j$, $G(Q) = \sum_{j=0}^{\infty} G_j$, $H(Q) = \sum_{j=0}^{\infty} H_j$, $K(Q) = \sum_{j=0}^{\infty} K_j$, and $J(Q) = \sum_{j=0}^{\infty} J_j$. The Adomian polynomials may be calculated in a variety of ways (Rach, Wazwaz, and Duan, 2013; Duan and Rach, 2011; Rach, 2008; Wazwaz, 2000; Adomian, 1994). Hence, (6) becomes

$$Q = Q_L x - L_x^{-1} \sum_{j=0}^{\infty} F_j L_t \sum_{i=0}^{\infty} Q_i + L_x^{-1} \sum_{j=0}^{\infty} G_j + \sum_{j=0}^{\infty} H_j + \sum_{j=0}^{\infty} K_j + L_x^{-1} \sum_{j=0}^{\infty} J_j L_t \sum_{i=0}^{\infty} Q_i \quad (8)$$

Defining the first term in the series, Q_k , as composed of the first two terms in the right side of (8),

$$Q_k = Q_L x - L_x^{-1} \sum_{j=0}^{\infty} F_j L_t \sum_{i=0}^{\infty} Q_i \quad (9)$$

Clearly, Q_k satisfies the kinematic wave equation given by

$$\frac{\partial Q_k}{\partial x} + \alpha \beta Q_k^{\beta-1} \left(\frac{\partial Q_k}{\partial t} \right) = Q_L, \quad Q_k(0,t) = Q_I(t), \quad Q_k(x,0) = Q_I(0) \quad (10)$$

To solve (10), we will extend the approach of Serrano (2006). The characteristics equation of (10) is determined by (Jeffrey, 2003)

$$\frac{dt}{dx} = \alpha\beta Q_k^{\beta-1} \tag{11}$$

and the compatibility condition is

$$\frac{dQ_k}{dx} = Q_L \tag{12}$$

Integrating (12) along a characteristic that passes through the point $(0, \xi)$ yields

$$Q_k(x, t) = Q_I(\xi) + Q_L x \tag{13}$$

Integrating the characteristic equation (11) gives

$$t = \alpha\beta Q_k^{\beta-1}(\xi)x + \xi \tag{14}$$

Using (13) to eliminate ξ , (14) yields an implicit solution to (10):

$$Q_k = Q_I \left(t - \alpha\beta(Q_k - Q_L x)^{\beta-1}x \right) + Q_L x = Q_I \left(t - F(Q_k - Q_L x)x \right) + Q_L x \tag{15}$$

To approximate an explicit solution to (15), we use the concept of double decomposition to expand $Q_k = \sum_{i=0}^{\infty} Q_{ki}$, and the initial term $Q_{k0} = \sum_{m=0}^{\infty} Q_{k0m}$ in the right side of (15) (Serrano, 2006; Adomian, 1994). Thus, the first term in (15) becomes

$$Q_{k0} = Q_I \left(t - F\left(\sum_{m=0}^{\infty} Q_{k0m} - Q_L x\right)x \right) + Q_L x \tag{16}$$

Now expand $F = \sum_{j=1}^{\infty} F_j$, where F_j is calculated using one of the many algorithms for the Adomian polynomials (Duan and Rach, 2011; Rach, 2008, Wazwaz, 2000). Using the traditional Adomian polynomials about an initial term $f_0 = Q_{k0} - Q_L x = Q_I(t) - Q_L x$ (Adomian, 1994), the first few terms are

$$\begin{aligned} F_0(f_0) &= F(f_0) \\ F_1(f_0) &= F_0(f_0) \frac{dF(f_0)}{df_0} \\ F_2(f_0) &= F_1(f_0) \frac{dF(f_0)}{df_0} + \frac{F_0(f_0)^2}{2!} \frac{d^2F(f_0)}{df_0^2} \\ F_3(f_0) &= F_2(f_0) \frac{dF(f_0)}{df_0} + F_1(f_0)F_2(f_0) \frac{d^2F(f_0)}{df_0^2} + \frac{F_1^3(f_0)}{3!} \frac{d^3F(f_0)}{df_0^3} \\ &\vdots \end{aligned} \tag{17}$$

Combining (16) and (17), we successively approximate Q_{k0} :

$$\begin{aligned} Q_{k00} &= Q_I \left(t - xF_0(f_0) \right) + Q_L x, & f_0 &= Q_I(t) - Q_L x \\ Q_{k01} &= Q_I \left(t - x[F_0(f_0) + F_1(f_0)] \right) + Q_L x, & f_0 &= Q_{k00}(x, t) - Q_L x \\ Q_{k02} &= Q_I \left(t - x[F_0(f_0) + F_1(f_0) + F_2(f_0)] \right) + Q_L x, & f_0 &= Q_{k01}(x, t) - Q_L x \\ &\vdots \end{aligned} \tag{18}$$

Note that each term, Q_{k0m} , is evaluated at the previous one, $Q_{k0m-1} - Q_L x$. The convergence of decomposition series has been rigorously established in the mathematical community (Gabet, 1994, 1993, 1992; Abbaoui and Cherruault, 1994, Cherruault, 1989, and Cherruault et al., 1992). A convergent decomposition series made of the first few terms usually provides an effective model in practical applications. In most applications of the ADM, the convergence rate is so high that only a few terms are needed to assure an accurate solution. Thus, if, for instance, Q_{k02} is a reasonable approximation to Q_{k0} , then

$$Q_k \approx Q_{k0} \approx Q_I \left(t - x[F_0(f_0) + F_1(f_0) + F_2(f_0)] \right) + Q_L x, \quad f_0 = Q_{k02}(x, t) - Q_L x \tag{19}$$

(19) is the first approximation to the dynamic wave equations (2) and (8). It also constitutes an approximate analytical solution to the nonlinear kinematic wave equation (10). Higher-order terms in (8) are given by

$$Q_i = L_x^{-1} G_j + H_j + K_j + L_x^{-1} J L_t Q_{i-1} \quad (20)$$

Similar to (17), the Adomian polynomials for the nonlinear functions G , H , K , and J in (7), (8), and (20) are sequentially generated about an initial term. The first term is given by

$$\begin{aligned} G_0 &= G(Q_I) \\ H_0 &= H(Q_k) \\ K_0 &= L(Q_k) \\ J_0 &= J(Q_I) \end{aligned} \quad (21)$$

From (20) and (21), we derive the first term of the solution:

$$Q_0 = Q_k + L_x^{-1} G_0 + H_0 + K_0 + L_x^{-1} J_0 L_t Q_I \quad (22)$$

The second term of the nonlinear functions is given by

$$\begin{aligned} G_1 &= Q_0 \frac{dG(g_0)}{dg_0} \\ H_1 &= Q_0 \frac{dH(h_0)}{dh_0} \\ K_1 &= Q_0 \frac{dK(k_0)}{dk_0} \\ J_1 &= Q_0 \frac{dJ(j_0)}{dj_0} \end{aligned} \quad (23)$$

where $g_0 = h_0 = k_0 = j_0 = Q_I$. From (20) and (23), we derive the second term of the solution:

$$Q_1 = L_x^{-1} G_1 + H_1 + K_1 + L_x^{-1} J_1 L_t Q_I \quad (24)$$

The third term of the nonlinear functions is given by

$$\begin{aligned} G_2(g_0) &= Q_1 \frac{dG(g_0)}{dg_0} + \frac{Q_0^2}{2!} \frac{d^2 G(g_0)}{dg_0^2} \\ H_2(h_0) &= Q_1 \frac{dH(h_0)}{dh_0} + \frac{Q_0^2}{2!} \frac{d^2 H(h_0)}{dh_0^2} \\ K_2(k_0) &= Q_1 \frac{dK(k_0)}{dk_0} + \frac{Q_0^2}{2!} \frac{d^2 K(k_0)}{dk_0^2} \\ J_2(j_0) &= Q_1 \frac{dJ(j_0)}{dj_0} + \frac{Q_0^2}{2!} \frac{d^2 J(j_0)}{dj_0^2} \end{aligned} \quad (25)$$

From (20) and (24), we derive the third term of the solution:

$$Q_2 = L_x^{-1} G_2 + H_2 + K_2 + L_x^{-1} J_2 L_t Q_I \quad (26)$$

The fourth term of the nonlinear functions is given by

$$\begin{aligned}
G_3 &= Q_2 \frac{dG(g_0)}{dg_0} + Q_1 Q_2 \frac{d^2 G(g_0)}{dg_0^2} + \frac{Q_1^3}{3!} \frac{d^3 G(g_0)}{dg_0^3} \\
H_3 &= Q_2 \frac{dH(h_0)}{dh_0} + Q_1 Q_2 \frac{d^2 H(h_0)}{dh_0^2} + \frac{Q_1^3}{3!} \frac{d^3 H(h_0)}{dh_0^3} \\
K_3 &= Q_2 \frac{dK(k_0)}{dk_0} + Q_1 Q_2 \frac{d^2 K(k_0)}{dk_0^2} + \frac{Q_1^3}{3!} \frac{d^3 K(k_0)}{dk_0^3} \\
J_3 &= Q_2 \frac{dJ(j_0)}{dj_0} + Q_1 Q_2 \frac{d^2 J(j_0)}{dj_0^2} + \frac{Q_1^3}{3!} \frac{d^3 J(j_0)}{dj_0^3}
\end{aligned} \tag{27}$$

From (20) and (24), we derive the fourth term of the solution:

$$Q_3 = L_x^{-1} G_3 + H_3 + K_3 + L_x^{-1} J_3 L_t Q_I \tag{28}$$

If the magnitude of Q_3 is smaller than a desired resolution, then $Q \approx \sum_{i=0}^3 Q_i$. Otherwise the calculation may be continued in as described above.

VERIFICATION WITH INDEPENDENT NUMERICAL SOLUTIONS

Exact analytical solutions of the nonlinear kinematic wave and the nonlinear dynamic wave equations are rare. We verify the ADM approximate analytical solutions derived above with the controlled numerical experiments conducted by Szymkiewicz (2010). Assuming $\alpha=5/3$, $\beta=3/5$, $Q_L=0$, $n=0.03$, $B=25m$, $S_0=0.0005$, and an inflow hydrograph given by

$$Q_I(t) = q_0 + (q_{\max} - q_0) \left(\frac{t}{t_{\max}} \right)^{1 - \frac{t}{t_{\max}}} \tag{29}$$

where $q_0=5m^3/s$, $q_{\max}=100m^3/s$, and $t_{\max}=4hour$. Figure 1 shows a comparison between a three-term analytical nonlinear kinematic wave equations (17)-(19) at $x=75km$, a linearized kinematic wave using an empirically matched coefficient, and the numerical hydrograph calculated by the modified finite element method according to Szymkiewicz (2010). Strictly speaking, the kinematic wave (10) becomes linear when $\beta=1$. However, this approach would produce a linear wave which is completely incorrect, since the predicted hydrograph would appear many hours after the true one (i.e., out of the view window in Figure 1). For this reason, many hydrologists treat the coefficient in (10), $a = \alpha\beta\bar{Q}^{\beta-1}$, as a calibration parameter for an average fixed \bar{Q} by trial and error. A fitted value of $a=1/6$ was used in Figure 1. This illustrates the difficulties associated with linearization and linear models: The parameter a in the linear hydrograph is subjectively fitted and not calculated from the channel properties, which limits the model use as a forecasting tool; the parameter a of the linear hydrograph has different dimensions from those of α and β in the nonlinear hydrograph, and thus they are not comparable; the linear hydrograph is simply a pure translation of the inflow hydrograph, that is to say, it does not the gradual transformation into a sharp rising front and flat recession observed in nature. For a detailed discussion about the effect of α and β on the shape of the nonlinear hydrograph see Serrano (2006). In contrast to the linear hydrograph, the time to peak calculated by the nonlinear analytical (ADM) and numerical methods is in excellent agreement. The nonlinear analytical solution seems to better preserve the peak magnitude, in agreement with kinematic wave theory. There appears to be some minor differences in the recession limb possibly because of numerical dissipation. However, the calculation of the nonlinear analytical hydrograph is easier and faster than the numerical one; it requires only a few lines in any standard mathematics software, such as Maple. It is interesting to note that the front of the propagating nonlinear kinematic wave becomes steeper. This occurs because the advection velocity in (10), $\alpha\beta\bar{Q}^{\beta-1}$, increases with the flow rate, Q , so that the wave peak moves faster than the lower portions. At some point, the propagating wave may breakdown. For this particular problem, the ADM kinematic wave solution shows signs of instability at prolonged distances of observation (e.g., greater than 100 km), and no smooth

profiles of a breaking wave were produced. This is an interesting topic for future research.

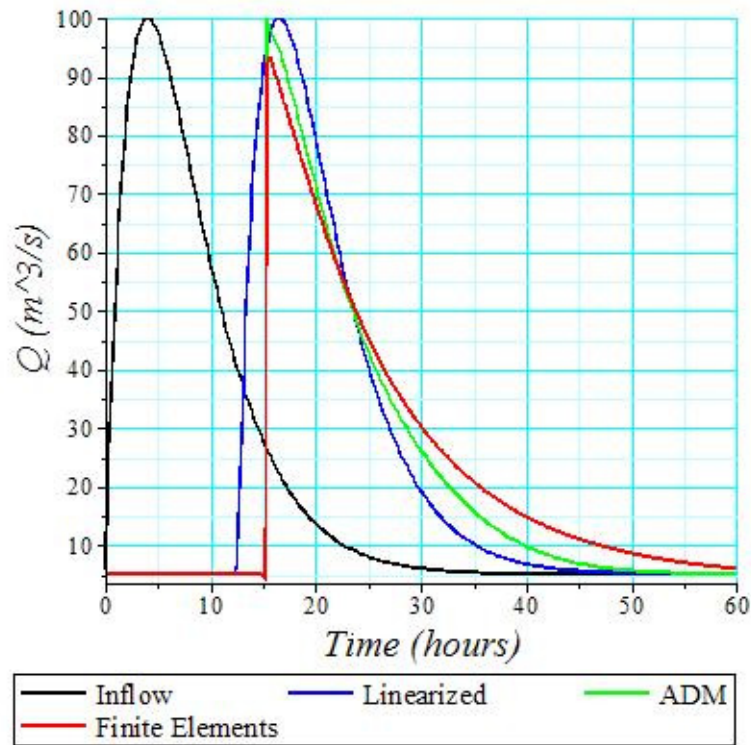


Figure 1: Analytical linear and nonlinear versus numerical nonlinear kinematic wave hydrograph at $x=75km$. Finite elements data kindly provided by Szymkiewicz (2010)

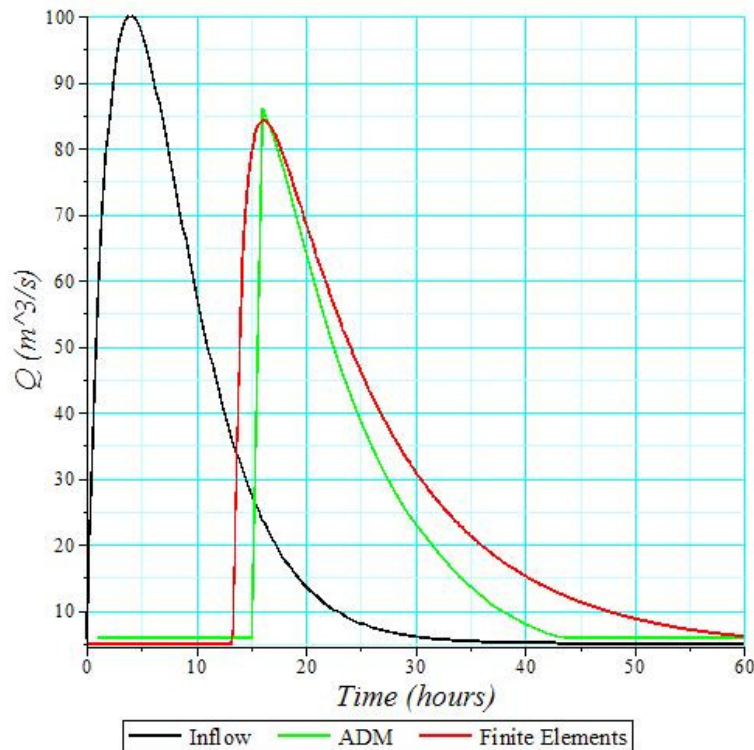


Figure 2: Analytical nonlinear dynamic wave versus numerical nonlinear diffusive wave hydrograph at $x=75km$. Finite elements data kindly provided by Szymkiewicz (2010)

Figure 2 shows a comparison between a four-term analytical nonlinear dynamic wave, equations (20)-(28), at $x=75\text{km}$ and the numerical diffusive hydrograph calculated by the modified finite element method according to Szymkiewicz (2010). The numerical hydrograph simulates the diffusion wave equation (i.e., it does not include all the terms of the momentum equation (2)). Nevertheless, it is interesting to note that the peak flow rate and the peak time are very similar in both hydrographs. Including the acceleration and pressure terms in the momentum equation causes a decrease in the magnitude of the flow rate at all times. Except for the flood peak, the nonlinear analytical solution exhibits lower flow rates than the numerical solution. The numerical solution also shows higher dispersion. In general, the ADM nonlinear kinematic and nonlinear dynamic wave solutions exemplify the usual features of nonlinear waves, namely its asymmetry with respect to its center of mass, with a sharp rising limb and a flatter recession limb. These features are usually missed by the linear methods. It is also interesting to observe that both the numerical and the analytical hydrographs exhibit errors in the balance of the transported quantity, a fact that has been known for a long time. In other words, the total volume of water leaving the river reach differs from that entering the channel, by about 6% for nonlinear kinematic wave models, 8% for nonlinear diffusion wave models, and perhaps greater for nonlinear dynamic wave models (Szymkiewicz, 2010). This is a limitation of the nonlinear models, independent of the method of solution used here. For more detailed analysis of mass and momentum conservation errors in simplified nonlinear models, see Szymkiewicz (2010).

FIELD VERIFICATION IN THE SCHUYLKILL RIVER IN SOUTHEAST PENNSYLVANIA

The new approximate analytical solutions to the nonlinear kinematic wave and the nonlinear dynamic wave equations were tested using data from the Schuylkill River in Southeast Pennsylvania. Major towns in the watershed include Pottsville, Reading, Pottstown, Norristown, Conshohocken, and Philadelphia. The river travels approximately 210 km from its headwaters at Tuscarora Springs in Schuylkill County to its mouth at the Delaware River in Philadelphia. The Schuylkill River is the largest tributary of the Delaware River and is a major contributor to the Delaware Estuary. Major tributaries of the Schuylkill, in downstream order, are Mill Creek, the West Creek, Perkiomen Creek, Wissahikon Creek, French Creek, and Tulpehocken Creek. The watershed encompasses an area of approximately 5,200 km^2 . The Schuylkill River has been an important source of drinking water in the region for over two centuries. Approximately 1.5 million people receive their drinking water from the Schuylkill River and its tributaries. For the purpose of this application, flow between the station at Norristown, with a watershed drainage area of 4,558 km^2 , and the station at Philadelphia, located 21km downstream and a drainage area of 4,903 km^2 are used. In this section, the river flows through a predominantly urban environment that includes residential, industrial, and commercial development. Discharge rate data at these stations are provided online by the U.S. Geological Survey, as described in the bibliography (U.S. Geological Survey, 2005). The same source provided individual discharge versus cross-sectional area data for the above stations. Using the information at these stations, we adopted the following average parameters: $B=150$; $n=0.014$, from the range of values suggested by Chow (1959) for rivers; $S_0=0.0006569$, as the average channel slope between the upstream and downstream stations; a rating-curve relationship of the form $A=\alpha Q^\beta$, where A is the channel wetted area (m^2), was fitted with average parameter values $\alpha=4.6 \text{ m}^{2-3\beta}\text{s}^\beta$, and $\beta=0.594$. The period of analysis included an unusually wet hydrologic year, beginning July 1, 2004.

To account for variable lateral flow, while maintaining a manageable, yet nonlinear, model, the lateral flow representation could be modified so as to account for the time variability of effective precipitation during high-intensity storms. For small sub-watersheds, the lateral inflow may be given as

$$Q_L(L,t)=q_0+\frac{cA_sP_e(t)}{L} \quad (30)$$

where $q_0=0.0001\text{m}^2/\text{s}$ is the constant lateral flow contribution from the groundwater flow estimated from the difference between average baseflow values at the downstream and the upstream stations, respectively; $A_s=3.45\times 10^8\text{m}^2$ is the watershed area between the monitoring stations; $L=21\text{km}$ is the distance along the stream between the upstream and downstream stations;

$c=0.2778 \times 10^{-6} \text{ m.mm}^{-1} \cdot \text{hour.s}^{-1}$ is a dimensions conversion factor; and $P_e(t)$ is the spatially-averaged effective precipitation rate in the sub-watershed obtained from daily rainfall rate estimates after the infiltration rate has been subtracted (mm/hour). Daily precipitation from rainfall was provided online by NOAA's National Climatic Data Center as described in the bibliography (National Oceanic and Atmospheric Administration NOAA, 2005). A constant loss rate of 75 mm/day was subtracted from the total daily rainfall values. In (30), consideration was not given to overland flow storage or surface routing effects.

Since the simulations used daily discharges reported at Norristown (inflow hydrograph, Q_I), a simplified version of the nonlinear kinematic and nonlinear dynamic wave equations was used. In other words, discharges at Philadelphia were approximated with a one-term decomposition term from (18) and (22):

$$\begin{aligned} Q &\approx Q_{k0} + L_x^{-1} G_0 + H_0 + K_0 + L_x^{-1} J_0 L_t Q_I \\ Q_{k0} &= Q_I (t - x F_0(f_0)) + Q_L x, \quad f_0 = Q_I(t) - Q_L x \end{aligned} \quad (31)$$

where the initial nonlinear functions F_0 , G_0 , H_0 , K_0 , and J_0 are given by (7), (17) and (21). Figure 3 displays a comparison between observed and predicted daily flow rates at Philadelphia for variable lateral inflow, according to the nonlinear dynamic wave (31), for the hydrologic year of 2004-2005. The inflow hydrograph at Norristown is not included for clarity. In general, agreement between the observed and predicted flow rates is reasonable. The inclusion of estimates of effective precipitation significantly improved the accuracy of the model with respect to observed flow rates, especially during peak times. The mean absolute error between observed and predicted discharge is $8.687 \text{ m}^3/\text{s}$ for the hydrologic year of 2004-2005. It is interesting to know that the greatest portion of the magnitude of discharge is given by the initial nonlinear kinematic wave component, Q_{k0} , which implies that in the lower Schuylkill river the translational components dominated the propagation of flood waves, in agreement with previous research (FEMA., 2014; Snyder Environmental Engineering Associates, 2007; Serrano, 2006). To better see this, a magnified detail of Figure 3 is depicted in Figure 4 illustrating the observed versus predicted discharge at Philadelphia with the nonlinear kinematic wave (19), using a one-term decomposition term in (18), and the nonlinear dynamic wave (31). The inflow at Norristown is not shown. In general, the nonlinear dynamic wave better predicts the flow rate, during peak times and especially during recession and low-flow periods. Thus, while both models are based on approximate analytical solutions and their implementation is easier than numerical solutions, the nonlinear kinematic wave equation model requires less data and could be useful in preliminary analyses with scarce data.

An additional set of tests of the new solutions was conducted in the same watershed during two different hydrologic years. The year of 2011 was an unusually wet year in the region and included the occurrence of Hurricane Irene. The next year, 2012, was not as wet, but it brought Hurricane Sandy to portions of the area. Figure 5 displays a comparison between observed and predicted daily flow rates at Philadelphia, according to the nonlinear dynamic wave (31), for the hydrologic year of 2011. The inflow hydrograph at Norristown is not shown for clarity. It is important to remark that no adjustment was made to the magnitude of any of the parameters. The mean absolute error between observed and predicted discharge was $16.490 \text{ m}^3/\text{s}$ for the year of 2011. Figure 6 shows a comparison between observed and predicted daily flow rates at Philadelphia, according to the nonlinear dynamic wave (31), for the year of 2012. The inflow hydrograph at Norristown is not shown for clarity. The mean absolute error between observed and predicted discharge was $8.540 \text{ m}^3/\text{s}$ for the year of 2012. Similar observations as those of the initial verification year of 2004 are noted.

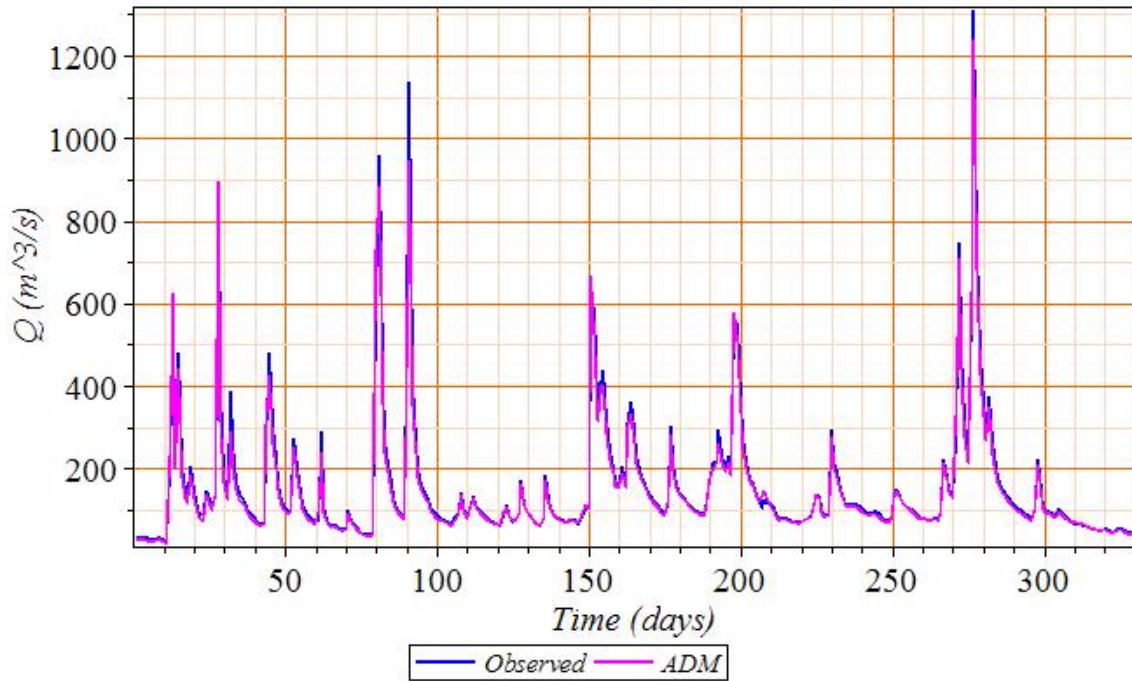


Figure 3: Observed versus predicted discharge at Philadelphia according to ADM analytical nonlinear dynamic wave during one hydrologic year beginning July, 2004

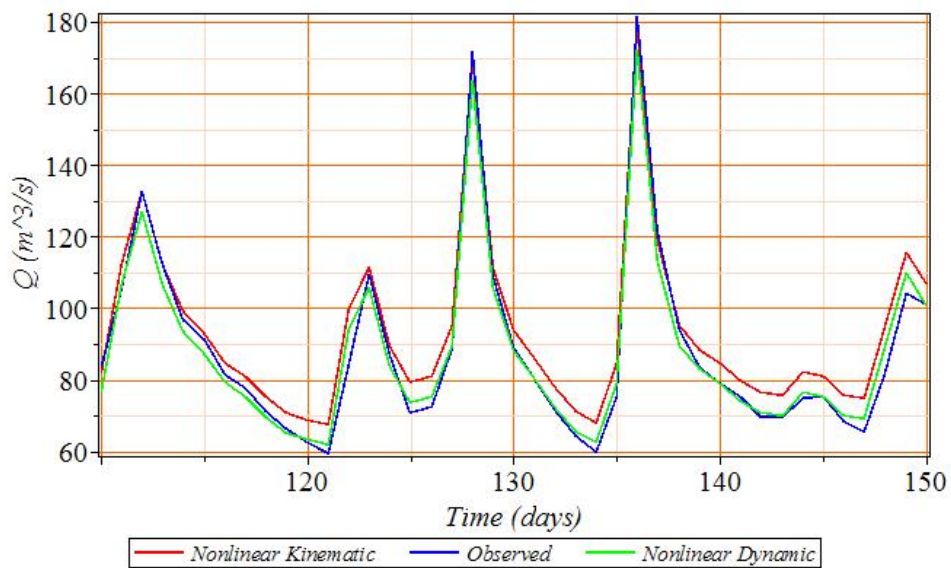


Figure 4: Detail of Figure 3 illustrating a comparison between observed versus predicted discharge at Philadelphia with the nonlinear kinematic wave and the nonlinear dynamic wave

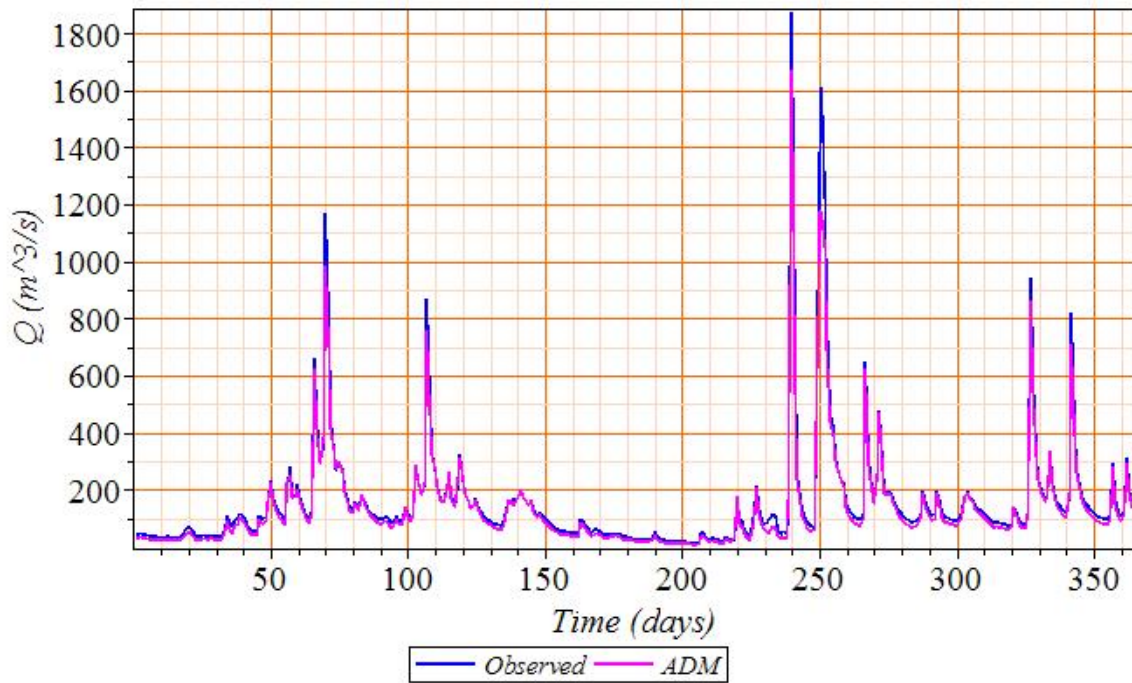


Figure 5: Observed versus predicted discharge at Philadelphia according to ADM analytical nonlinear dynamic wave during one hydrologic year beginning January, 2011

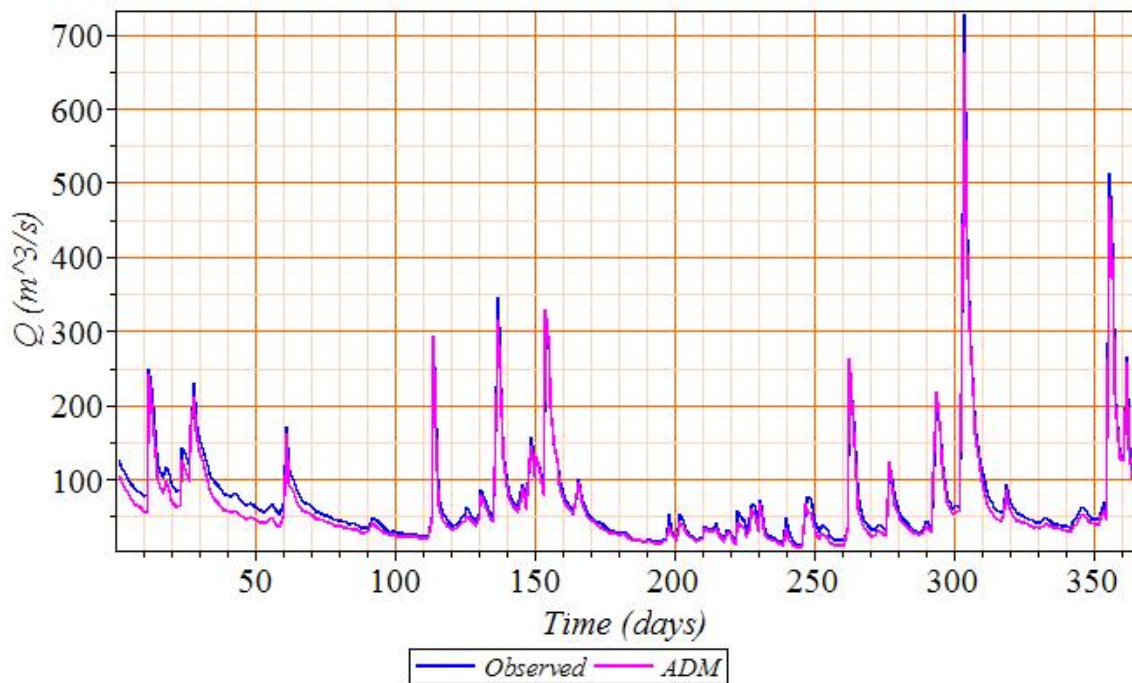


Figure 6: Observed versus predicted discharge at Philadelphia according to ADM analytical nonlinear dynamic wave during one hydrologic year beginning January, 2012

SUMMARY AND CONCLUSIONS

New approximate analytical solutions to the nonlinear kinematic wave equation and the nonlinear dynamic wave equation in rivers are compared with independent simulations using the modified finite-element method and with field data at the Schuylkill River near Philadelphia for the hydrologic year of 2004. The new solutions are further validated in the same watershed, without changing the parameters, for the hydrologic years of 2011 and 2012, when Hurricane Irene and Hurricane Sandy, respectively, touched down in the region. The new solutions compared favorably. The solutions were derived by combining Adomian's Decomposition Method (ADM), the method of characteristics, the concept of double decomposition, and successive approximation. The new solutions are easier to apply than numerical solutions, and permit the efficient forecast of nonlinear kinematic and nonlinear dynamic flood waves. Advantages include a simplified approach for preliminary hydrologic forecast under scarce data; an analytic description of flow rates and gradients; a description of state variables continuously over the spatial and temporal domain; minimal complications from stability and numerical roundoff; no need of a numerical grid or the handling of large sparse matrices; no need of specialized software, since all calculations may be done with standard mathematics or spreadsheet programs. The new solutions may also serve as a potential source of reference data for testing new numerical methods and algorithms proposed for the open channel flow equations. In general, the ADM nonlinear kinematic and nonlinear dynamic wave solutions exhibit the usual features of nonlinear waves, namely its asymmetry with respect to its center of mass, with sharp rising limbs and flatter recession limbs. Linear approximations of the governing equations usually miss these important features of nonlinear waves. The greatest portion of the magnitude of discharge is given by the initial nonlinear kinematic wave component, Q_{k0} , which implies that in the lower Schuylkill river the translational components dominate the propagation of flood waves, in agreement with previous research. The nonlinear dynamic wave better predicts the flow rate, during peak times and especially during recession and low-flow periods. Thus, while both the nonlinear kinematic and the nonlinear dynamic wave models are based on approximate analytical solutions and their implementation is easier than numerical solutions, the nonlinear kinematic wave equation model requires less data and less computational effort.

BIBLIOGRAPHY

- Abbaoui, K., and Cherruault, Y., 1999. Convergence of Adomian's Method Applied to Differential Equations. *Comp. Math. Applic.*, 28(5):103-109.
- Adomian, G., 1995. Analytical Solution of Navier-Stokes Flow of a Viscous Compressible Fluid. *Foundations of Physics Letters*, 8(4):389-400.
- Adomian, G., 1994. *Solving Frontier Problems in Physics-The Decomposition Method*. Kluwer Acad. Pub.
- Adomian, G., 1991, A Review of the Decomposition Method and Some Recent Results for Nonlinear Equations. *Comp. Math. Applic.* 21(5), 101-127.
- Adomian, G., 1983. *Stochastic Systems*. Academic Press, New York.
- Aronica, G., Tucciarelli, T., and Nasello, C., 1998. 2D Multilevel Model for Flood Wave Propagation in Flood-affected Areas. *ASCE J. Water Resour. Plan. Manage.*, 124, 210–217, doi:10.1061/(ASCE)0733-9496(1998)124:4(210).
- Bates, P. D., Horritt, M. S., and Fewtrell, T.J., 2010, a Simple Inertial Formulation of the Shallow Water Equations for Efficient Two-dimensional Flood Inundation Modelling. *J. Hydrol.*, 387, 33–45, doi:10.1016/j.jhydrol.2010.03.027.
- Beven, K., 2006. Searching for the Holy Grail of Scientific Hydrology: $Q_t = (S, R, t)A$ as Closure. *Hydrol. Earth Syst. Sci.*, 10, 609-618, doi:10.5194/hess-10-609-2006.
- Beven, K., 2001. How Far Can We Go in Hydrological Modelling, *Hydrol. Earth Sys. Sci.*, 5(1), 1-12.
- Cappelaere, B., 1997. Accurate Diffusive Wave Routing. *ASCE J. Hydraul. Eng.*, 123(3), 174–181.
- Cherruault, Y., 1989. Convergence of Adomian's Method. *Kybernetes*, 18(2):31-38.
- Cherruault, Y., Saccomardi, G., and Some, B., 1992. New Results for Convergence of Adomian's Method Applied to Integral Equations. *Math. Comput. Modelling*, 16(2):85-93.
- Chow, V. T., 1959. *Open Channel Hydraulics*. McGraw-Hill Kogakusha, Ltd., Tokyo.
- Chow, V.T., Maidment, D.R., and Mays, L.W., 1988. *Applied Hydrology*. McGraw-Hill Book Co., New York.

- de Almeida, G. A. M., and Bates, P., 2013. Applicability of the Local Inertial Approximation of the Shallow Water Equations to Flood Modeling. *Water Resour. Res.*, 49: 4833–4844, doi:10.1002/wrcr.20366.
- de Almeida, G. A. M., Bates, P. D., Freer, J., and Souvignet, M., 2012. Improving the Stability of a Simple Formulation of the Shallow Water Equations for 2d Flood Modelling. *Water Resour. Res.*, 48, doi:10.1029/2011WR011570.
- Di Silvio, G., 1969. Flood Wave Modification along Prismatic Channels. *ASCE J. Hydraul. Div.*, 95, 1589–1614.
- Dooge, J. C. I., and Napiorkowski, J. J., 1987. Applicability of Diffusion Analogy in Flood Routing. *Acta Geophys. Pol.*, 35(1), 65–75.
- Duan, J. -S, and Rach, R., 2011. A New Modification of the Adomian Decomposition Method for Solving Boundary Value Problems for Higher-Order Nonlinear Differential Equations. *Appl. Math. Comput.*, 218:4090-4118.
- FEMA, 2014. Flood Risk in the Schuylkill Watershed. U. S. Department of Homeland Security. www.delawareriverkeeper.org Accessed July, 2015.
- Ferrick, M. G., 1985. Analysis of River Wave Types, *Water Resour. Res.*, 21(2), 209–220, doi:10.1029/WR021i002p00209.
- Ferrick, M. G., Bilmes, J., and Long, S.E., 1984. Modeling Rapidly Varied Flow in Tailwaters. *Water Resour. Res.*, 20(2), 271–289, doi:10.1029/WR020i002p00271.
- Gabet, L., 1994. The Decomposition Method and Distributions. *Computers Math. Applic.*, 27(3):41-49.
- Gabet, L., 1993. The Decomposition Method and Linear Partial Differential Equations. *Math. Comput. Modelling*, 17(6):11-22.
- Gabet, L., 1992. *Equisse D'une Théorie Décompositionnelle et Application Aux Equations Aux Dérivées Partielles*. Dissertation, Ecole Centrale De Paris, France.
- Hromadka, T. V. and Yen, C. C., 1986. A Diffusion Hydrodynamic model (DHM). *Adv. Water Resour.*, 9, 118–121.
- Jeffrey, A., 2003. *Applied Partial Differential Equations*. Academic Press, NY.
- Jin, M. and Fread, D. (1997). Dynamic Flood Routing with Explicit and Implicit Numerical Solution Schemes. *ASCE J. Hydraul. Eng.*, 123(3), 166–173.
- Kazezyilmaz-Alhan, C. and Medina, M., Jr. (2007). Kinematic and Diffusion Waves: Analytical and Numerical Solutions to Overland and Channel Flow. *ASCE J. Hydraul. Eng.*, 133(2), 217–228.
- Lamberti, P., and Pilati, S, 1996. Flood Propagation Models for Real-time Forecasting. *J. Hydrol.*, 175, 239–265.
- Lighthill, M. J., and Whitham, G. B., 1955. On Kinematic Waves. I. Flood Movement in Long Rivers. *Proc. R. Soc. London, Ser. A*, 229, 281–316, doi:10.1098/rspa.1955.0088.
- Litrico, X., and Guinot, V., 2007. “Discussion of ‘Development and Verification of an Analytical Solution for Forecasting Nonlinear Kinematic Flood Waves.’” *ASCE J. Hydrol. Eng.*, 12(6):703-705.
- Martin, J. L. And McCutcheon, S.C., 1999. *Hydrodynamics and Transport for Water Quality Modeling*. Lewis Publishers, Boca Raton, FL.
- Moramarco, T., Pandolfo, C, and Singh, V. P., 2008. Accuracy of Kinematic Wave and Diffusion Wave Approximations for Flood Routing. I: Steady Analysis. *ASCE J. Hydrologic Eng.*, 13(11), 1089–1096.
- Morris, E. M., and Woollhiser, D. A., 1980. Unsteady One-dimensional Flow over a Plane: Partial Equilibrium and Recession Hydrographs. *Water Resour. Res.*, 16(2), 355–360.
- National Oceanic and Atmospheric Administration NOAA, 2005. NOAA National Climatic Data Center, <http://www.ncdc.noaa.gov>
- Philipp, A., Liedl, R., and Wöhling, T., 2012. Analytical Model of Surface Flow on Hillslopes Based on the Zero Inertia Equations. *ASCE J. Hydraul. Eng.*, 138(5), 391–399, doi:10.1061/(ASCE)HY.1943-7900.0000519.
- Ponce, V. M., 1986. Diffusion Wave Modelling of Catchment Dynamics. *ASCE J. Hydraul. Eng.*, 112(8), 716–727.
- Ponce, V. M. and Chaganti, P. V. (1994). VPM-Cunge Revisited. *J. Hydrol*, 162(3-4), 517 433-439.
- Ponce, V. M., Li, R.-M., and Simons, D. B., 1978. Applicability of Kinematic and Diffusion Models. *ASCE J. Hydraul. Div.*, 104(HY3), 353–360.
- Ponce, V. M., and Simons, D. B., 1977. Shallow Wave Propagation in Open Channel Flow. *ASCE J. Hydraul. Div.*, 103(HY12), 1461–1476.

- Price, R., K., 2009. Volume-Conservative Nonlinear Flood Routing. *ASCE J Hydraul. Engr.*, 135(10):838-845.
- Rach, R., 2012. A Bibliography of the Theory and Applications of the Adomian Decomposition Method, 1961-2011. *Kybernetes*, 41(7/8):1087-1148.
- Rach, R., 2008. A New Definition of the Adomian Polynomials. *Kybernetes*, 37(7):910-955.
- Rach, R., Wazwaz, A. -M., and Duan, J. -S., 2013. A Reliable Modification of the Adomian Decomposition Method for Higher-order Nonlinear Differential Equations. *Kybernetes*, 42(2):282-308.
- Reggiani, P., Todini, E., and Meißner, E., 2014. A conservative Fow Routing Formulation: Déjà vu and the Variable-parameter Muskingum Method Revisited. *J. Hydrol.*, 11(519):1506-1515.
- Serrano, S.E., 2006. Development and Verification of an Analytical Solution for Forecasting Nonlinear Kinematic Flood Waves. *ASCE Journal of Hydrol. Eng.*, 11(4):347-353.
- Serrano, S. E., 2007. Closure to “Development and Verification of an Analytical Solution for Forecasting Nonlinear Kinematic Flood Waves” by Sergio E. Serrano. *ASCE J. Hydrologic Eng.*, 12(6):705-707.
- Serrano, S.E., 2011. *Engineering Uncertainty and Risk Analysis. A Balanced Approach to Probability, Statistics, Stochastic Models, and Stochastic Differential Equations.* 2nd Ed., HydroScience Inc., Ambler, PA.
- Serrano, S.E., 2010. *Hydrology for Engineers, Geologists, and Environmental Professionals. An Integrated Treatment of Surface, Subsurface, and Contaminant Hydrology.* 2nd Ed., HydroScience, Inc. Ambler, PA.
- Serrano, S. E., 2016. Propagation of Nonlinear Flood Waves in Rivers. *ASCE Journal of Hydrologic Engineering*, 21(1):04015053:1-7. [http://dx.doi.org/10.1061/\(ASCE\)HE.1943-5584.0001268](http://dx.doi.org/10.1061/(ASCE)HE.1943-5584.0001268)
- Singh, V.P., 1996. *Kinematic Wave Modeling in Water Resources: Surface Water Hydrology.* Wiley, NY.
- Singh, V. P., and Aravamuthan, V. 1996. Errors of Kinematic-Wave and Diffusion-Wave Approximations for Steady-state Overland Flows. *Catena*, 27(3–4), 209–227.
- Snyder Environmental Engineering Associates, 2007. *Analysis of Hydraulic Impacts on the Schuylkill River Manayunk Sewer Basin Construction Project and the Venice Island Recreation Center Reconstruction Project Venice Island, Manayunk, Philadelphia, PA.* Accessed July, 2015.
www.manayunkcouncil.org/zoning/VI-Lower/20070912-hydrolic-analysis.pdf
- Szymkiewicz, R., 2010. *Numerical Modeling in Open Channel Hydraulics.* Water Science and Technology Library. Springer, New York, NY.
- Todini, E. (2007). A mass Conservative and Water Storage Consistent Variable Parameter Muskingum-Cunge Approach. *Hydrol. Earth Syst. Sci.*, 11, 1645-1659, 558 doi:10.5194/hess-11-1645-2007.
- Tsai, C. W., and Yen, B.C., 2004. Shallow Water Propagation in Convectively Accelerating Open-channel Flow Induced by Tailwater Effect. *ASCE J. Eng. Mech.*, 130(3), 320–336.
- Tsai, C. W., 2003. Applicability of Kinematic, Noninertia, and Quasi-steady Dynamic Wave Models to Unsteady Flow Routing. *ASCE J. Hydraul. Eng.*, 129(8), 613–627.
- U.S. Geological Survey, 2005. NWIS Site Inventory for the U.S.A., <http://waterdata.usgs.gov/nwis>
- Vieira, J. H. D., 1983. Conditions Governing the Use of Approximations for the Saint-venant Equations for Shallow Surface Water Flow. *J. Hydrol.*, 60, 43–58.
- Wazwaz, A.-M., 2000. A New Algorithm for Calculating Adomian Polynomials for Nonlinear Operators. *Appl. Math. Comput.*, 111:53-69.
- Woolhiser, D. A., and Liggett, J. A., 1967. Unsteady, One-dimensional Flow over a Plane—the Rising Hydrograph. *Water Resour. Res.*, 3(3), 753–771, doi:10.1029/WR003i003p00753.
- Xia, R., 1995. Impact of Coefficients in Momentum Equation on Selection of Inertial Models. *J. Hydraul. Res.*, 32(4), 615–621.

Acknowledgments

Numerical data for the comparison of the ADM models in Figures 1 and 2 was kindly provided by Professor Romuald Szymkiewicz from the Gdańsk University of Technology, Poland (Szymkiewicz, 2010, pp. 377-379). Streamflow data for the present study was provided online by the U.S. Geological Survey (U.S. Geological Survey, 2005. NWIS Site Inventory for the U.S.A., <http://waterdata.usgs.gov/nwis>). Rainfall information for the present study was provided online by the U.S. National Oceanic and Atmospheric Administration National Oceanic and Atmospheric Administration NOAA, 2005 (NOAA National Climatic Data Center, <http://www.ncdc.noaa.gov>).